The microfabric of calcite tectonites from the Helvetic Nappes (Swiss Alps)

S. M. Schmid, M. Casey & J. Starkey

SUMMARY: The crystallographic orientations of calcite in tectonites from the Morcles Nappe and the Glarus Overthrust have been measured by X-ray texture goniometry. The orientation data are represented by pole figures, inverse pole figures and as orientation distribution functions.

The patterns of preferred orientation observed in the specimens from the Morcles Nappe are correlated with intracrystalline slip mechanisms. The patterns exhibit quasi-axial symmetry and in some cases the axis of symmetry is oblique to the symmetry of the macroscopic fabric. This obliquity is interpreted as the result of a rotational strain path and may be used to infer direction and sense of shear.

Some specimens of the Lochseiten mylonite from the Glarus Thrust show no strong preferred crystallographic orientation. This suggests that grain boundary sliding was the major deformation mechanism.

The crystallographic orientation (texture) of experimentally deformed limestones has been measured by X-ray methods for specimens deformed within a wide range of experimental conditions (Wenk *et al.* 1973; Casey *et al.* 1978). It is tempting, therefore, to compare the observed textures with those from naturally deformed limestones. The limestones of the Helvetic Nappes, deformed at temperatures estimated to be not higher than 400°C offer such an opportunity because they have not been annealed after deformation and are therefore likely to have preserved a syntectonic microfabric.

Samples were collected from (1) the area of the Morcles Nappe in W Switzerland and (2) along the Glarus Overthrust in E Switzerland (Table 1). The Morcles Nappe has an inverted limb where the stratigraphic sequence is preserved in spite of a drastic thickness reduction of as much as 1:100 (Badoux 1972). Along the Glarus Overthrust an extremely thin mylonitic layer (1 m thick, Schmid 1974), has been completely detached from its original substratum and sandwiched between two thrust blocks.

X-ray texture goniometry

Apparatus and data analysis

The specimens were analysed with the combined reflection and transmission scan method (Siddans 1976) using Co K_α radiation. A computer controlled texture goniometer built by Seiffert-Scintag was used for the analysis. For the specimens presented in Fig. 1, eight reflections of calcite were measured (see Casey

TABLE 1. *Localities of analysed specimens*

Specimen No.	Lithology	Locality
7816	fine-grained limestone (Dogger)	Inverted limb Morcles Nappe, near Saillon
7822	white, fine-grained marble (Urgonian)	Inverted limb Morcles Nappe, near Saillon
71	limestone conglomerate (Tertiary)	Inverted limb Morcles Nappe, SE Dents de Morcles
63	Lochseiten mylonite	Foostock
6	Lochseiten mylonite	Lochseite
115	Lochseiten mylonite	Ringelspitz

The dip azimuth of both lineations and foliations is SSE–ESE in the Morcles area. For the Lochseiten mylonites with a subhorizontal foliation the transport direction was assumed to be towards the N, based on field geological evidence.

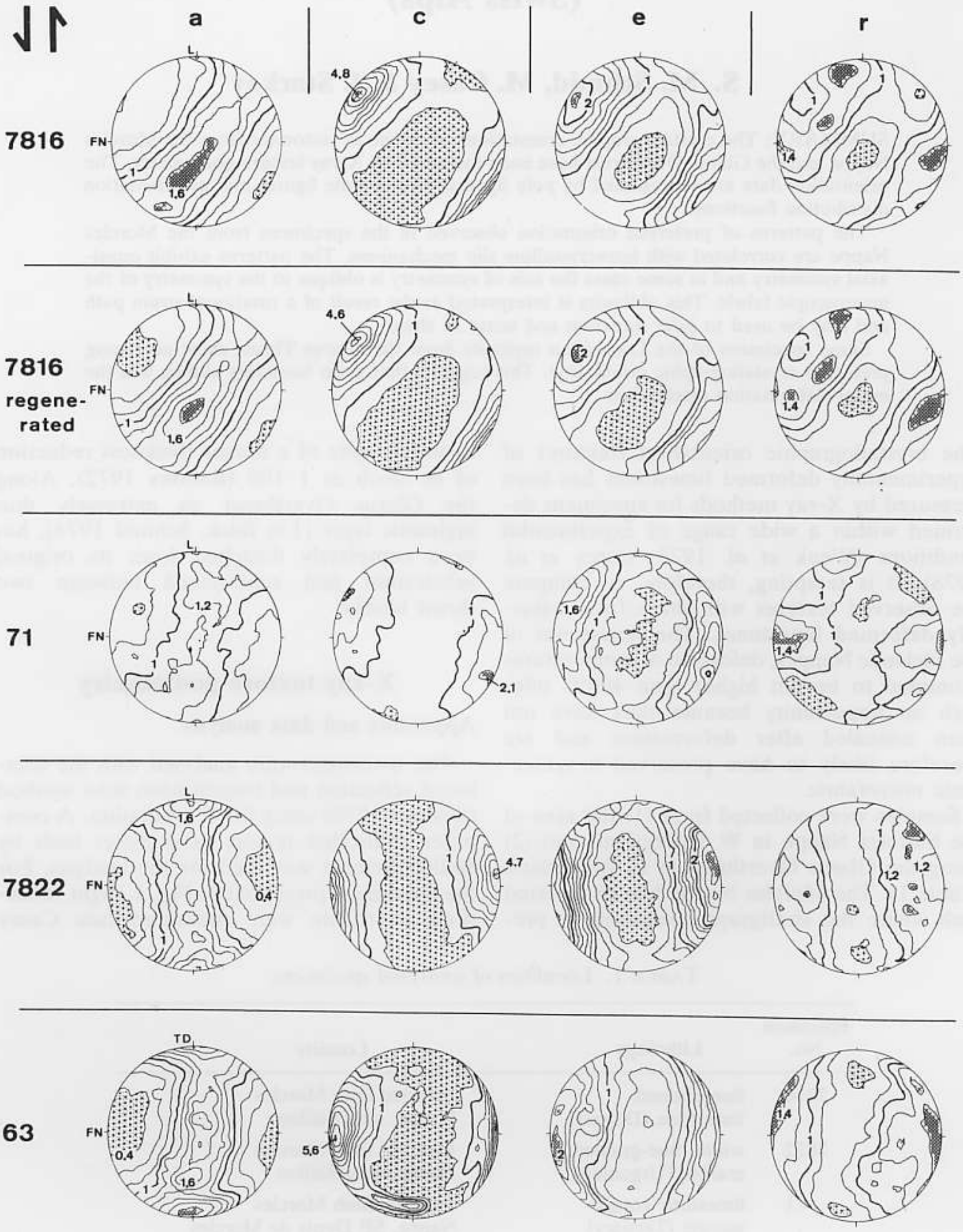

FIG. 1. Pole figures for selected crystallographic directions for some of the specimens studied. The regenerated pole figures for specimen 7816 (degree of expansion 16) are included for comparison with the measured data. Contour intervals for the *a*, *e* and *r* patterns are 0.2 times uniform, contour intervals for *c* are 0.5. FN indicates the position of the foliation normal, L the lineation and TD the transport direction.

et al. 1978, table 1). The counting time was 50 s. for each 5° step in the azimuth and tilt and 100 s on two background positions after every increment in tilt (for the weak *c*-reflection counting times were doubled). The defocussing correction in reflection mode is based on calibrations using a limestone with no preferred orientation kindly provided by H. Siemes, Aachen.

For the calculations of the orientation distribution function (O.D.F.) the digital data were transferred to a CDC-computer. The programs used are based on the methods of Bunge (1969) and Bunge & Wenk (1977). The orientation distribution function is represented as a series of generalized spherical harmonic functions and the pole figures and inverse pole figures are represented as series of spherical surface harmonics. Linear relationships exist between the coefficients of the pole figure and the orientation distribution series expansions. Once sufficient pole figures have been measured and expressed as spherical harmonic expansions, the orientation distribution function coefficients may be calculated. From these coefficients it is possible to calculate serial sections through the O.D.F., to calculate inverse pole figures and to calculate pole figures for any diffracting plane. In Fig. 1 a set of pole figures recalculated from the O.D.F. gives an indication of the consistency of the input data. The programs used are general and handle triclinic specimen symmetry (Casey, unpubl. manuscript 1979).

Graphical representation of texture data

The three representations of texture data used in Figs 1–3 are briefly introduced here, for further discussion see Bunge (1969) and Bunge & Wenk (1977).

Pole figures (Fig. 1)

The preferred orientation of a particular crystal direction is represented in an upper hemisphere equal area projection with respect to specimen coordinates. The specimen X axis (X_s) was chosen parallel to the lineation or supposed transport direction (labelled L and TD respectively in Fig. 1), Y_s is parallel to the foliation normal (labelled FN) and Z_s is in the centre of the pole figure. All pole figures in Fig. 1 are oriented such that the sense of shear as inferred from field geological evidence is sinistral. The orientation patterns are contoured in multiples of a uniform distribution.

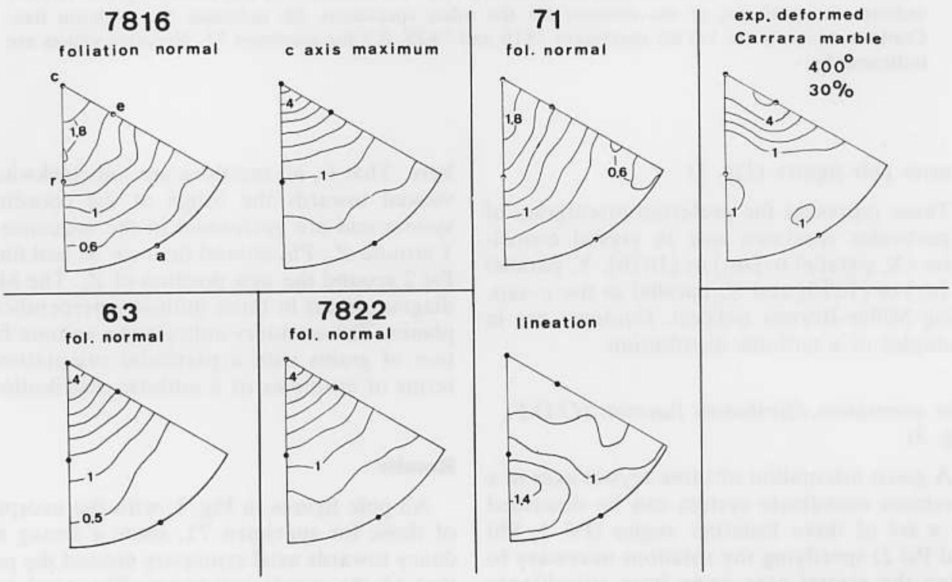

Fig. 2. Inverse pole figures for selected specimen directions (degree of expansion 16). Contour intervals are 0.2 for specimens 7816 (foliation normal) and specimen 71; 0.5 for specimens 63, 7822 and the *c*-axis maximum of 7816; 1.0 for the experimentally deformed marble (from Casey *et al.* 1978).

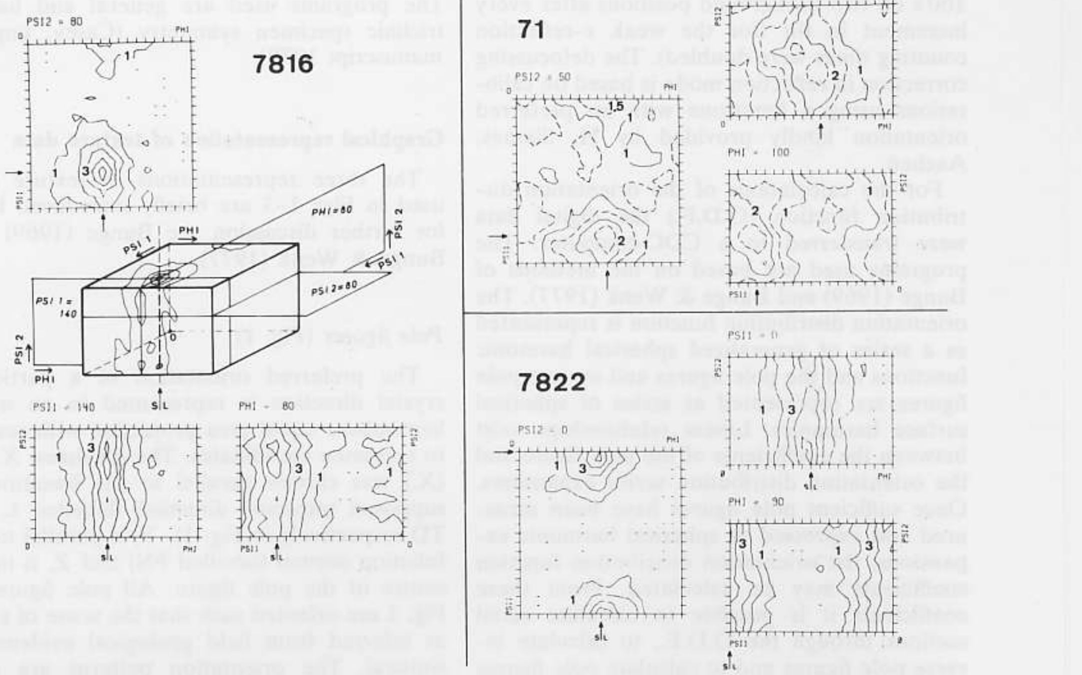

FIG. 3. Three mutually perpendicular sections through the orientation distribution function of selected specimens (degree of expansion 12 for specimens 71 and 7822, degree 16 for specimen 7816). The positions of the sections for specimen 7816 are indicated by the block diagram. Arrows indicate the positions of the sections for the other specimens, SL indicates the skeleton line. Contour intervals are 1.0 for specimens 7816 and 7822; 0.5 for specimen 71. Negative values are indicated by - .

Inverse pole figures (*Fig. 2*)

These represent the preferred orientation of a particular specimen axis in crystal coordinates (X_c parallel to $[m_1]$ or $[10\bar{1}0]$, Y_c parallel to $[a_2]$ or $[\bar{1}2\bar{1}0]$ and Z_c parallel to the c-axis, using Miller-Bravais indices). Contours are in multiples of a uniform distribution.

The orientation distribution function (*O.D.F., Fig. 3*)

A given orientation of three crystal axes in a specimen coordinate system can be described by a set of three Eulerian angles (Psi 1, Phi and Psi 2) specifying the rotations necessary to bring the crystal axes away from coincidence with the specimen axes and into their actual position. This orientation can be represented by a point in a block diagram, Fig. 3. The convention of Bunge (1969, fig. 2.5) is used here. That is, all rotations are anticlockwise as viewed towards the origin of the coordinate system and are performed in the sequence Psi 1 around Z_c, Phi around the new X_c and finally Psi 2 around the new position of Z_c. The block diagram is cut in three mutually perpendicular planes. The contours indicate the volume fraction of grains with a particular orientation in terms of multiples of a uniform distribution.

Results

All pole figures in Fig. 1, with the exception of those for specimen 71, show a strong tendency towards axial symmetry around the position of the c-axis maximum. The axial symmetry is not perfect because the e-poles form a point maximum rather than a 26° small circle as expected for perfect symmetry. This departure from axial symmetry may be seen in the inverse pole figure for the direction of the c-axis maximum of specimen 7816 (Fig. 2): the contours deviate from ideal circles and a very weak ridge towards e is developed. Specimen 7822 shows the closest approach to axial symmetry (Fig. 2).

The c-axis maxima of specimens 63 and 7822 (Fig. 1) coincide approximately with the foliation normal but in specimens 71 and 7816 the maxima are displaced from the foliation normal by 30°, in the case of specimen 71 and 40° for specimen 7816. In both cases the displacement is clockwise from the foliation normal, that is to say in a sense opposite to the sense of shear. The contours for c and e in specimen 63 (to a smaller extent also in 7816 and 71) in Fig. 1 depart from small circles around the point maximum and the high concentration areas are elongated in the plane of projection (X–Z plane of the finite strain ellipsoid).

A more complex set of pole figures was obtained from specimen 71. There is a relatively strong r-maximum near the foliation normal and a secondary maximum near the lineation (compare the well developed r-shoulder in the inverse pole figure for the foliation normal of this specimen in Fig. 2). The inverse pole figure for the lineation in 71 shows a maximum near $\langle r_2 : r_3 \rangle$ (Fig. 2).

The orientation distribution functions for both specimens 7816 and 7822 (Fig. 3) are characterized by a cylindrical zone of higher concentration (skeleton line, Bunge 1969) parallel to the Psi 2 axis. This reflects the high degree of axial symmetry around the c-axis maximum (no preference for a particular rotation angle Psi 2 around the final position of the c-axis). Note that the position of the skeleton line in the Pse 1–phi plane is different for specimens 7816 and 7822. This is an expression of the different position of the c-axis maximum relative to specimen coordinates in these two specimens.

Specimen 71 shows a more complex O.D.F. with a less clearly developed skeleton line and a preference for Psi 2 to lie between 40° and 90°. This corresponds to at least 2 out of the 3 r-poles lying nearly at 90° to the lineation and near the foliation normal, the third r-pole is parallel to the secondary maximum of the r-pole figure (compare Fig. 1).

Two additional specimens of Lochseitenkalk were measured (specimens 6 & 115, Table 1). Their orientation patterns were indistinct and weak relative to those already described, for instance the maximum concentration of the e orientation pattern for specimen 6 is less than 1.6 times uniform, the maximum for 115 is less than 1.4.

Microstructure

Morcles area

In specimens 7816 and 71 the matrix grains are elongated, with axial ratios up to 1:1.5, in a plane which is oblique to the foliation by 50° in 7816, and variable up to 25° in 71, Fig. 4. The shorter axes of the grains are therefore nearly parallel to the c-axis maximum in these specimens rather than perpendicular to the foliation. It should be mentioned at this point that foliation is macroscopically well developed as a good rock cleavage in all the specimens. In the case of specimen 71 conglomerate pebble shapes with an estimated axial ratio of 50:10:1 (pers. comm. J. Barber) indicate that the macroscopic foliation is apparently parallel to the principal plane of flattening in the finite strain ellipsoid.

Specimens 7816 and 71 have grain sizes between 5 and 30 μm, while specimen 7822, the marble, is only slightly coarser grained (10–50 μm). Specimen 7816 is free of larger calcite intraclasts; specimens 71 and 7822 contain a few isolated intraclasts up to 0.5 mm diameter (Fig. 4b), making up less than 10% of the rock volume. In specimens 7816 and 7822 e-twins are abundant and broad, undulose extinction and bent twins indicate that dislocation glide systems were active. In specimen 71 however, only a few twins are visible in the intraclasts and the matrix grains are free from twinning. The intraclasts of this latter specimen contain deformation bands in the grain interior and equiaxial subgrains near the grain boundary (Fig. 4b). These subgrains have the same diameter as the matrix grains, suggesting that syntectonic recrystallization by subgrain rotation may have lead to the fine-grained mosaic of matrix grains with straight and well equilibrated grain boundaries, which are typical for both specimens 71 and 7822. Specimen 7816, however, exhibits very serrated grain boundaries indicative of grain boundary migration.

Glarus area

Specimen 63 of Lochseiten mylonite shows no macroscopically visible lineation. The microstructure is different from that observed in the rocks from Morcles (Fig. 4d): large, twinned and extremely intensely strained intraclasts occur in a very much finer grained matrix (less than a few μm). The matrix grains are

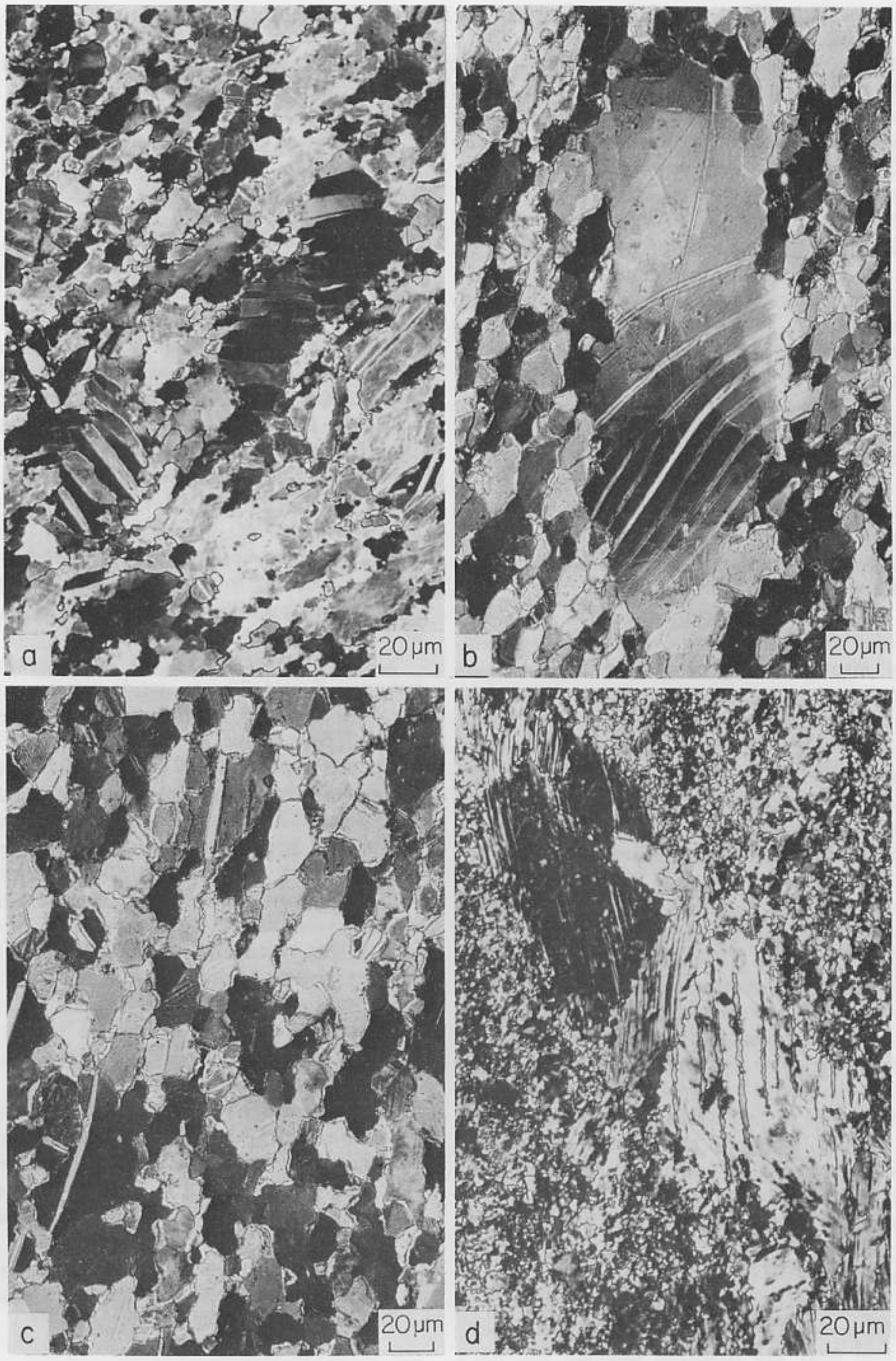

FIG. 4. For all photomicrographs the macroscopic foliation is N–S and perpendicular to the plane of section, the supposed sense of shear is sinistral. The orientation of the photomicrographs therefore corresponds to that of the pole figures of Fig. 1. (a) Specimen 7816; note broad deformation twins and serrated grain boundaries; the plane of mean grain elongation is oblique to the foliation. (b) Specimen 71; note deformation bands and subgrains in the larger intraclast which are flattened in the plane of foliation. Note however that the matrix grains are flattened in a plane oblique to the foliation. (c) Specimen 7822; mosaic of grains with equilibrated grain boundaries. (d) Specimen 63; large intraclasts with deformation twins preferentially oriented parallel to the foliation in a very fine-grained recrystallized matrix.

equiaxial. U-stage measurements on intraclasts indicate a very strong preferred orientation of the c-axes perpendicular to foliation. This, together with the observation that specimens 6 and 115 with their weak textures contain no such intraclasts, suggests that the strong texture of specimen 63 may be attributed solely to the intraclasts which make up about one third of the rock volume.

Discussion and conclusions

The well established slip systems for calcite are e-twinning, r-glide and f-glide (see review by Carter 1976). Experimental deformation of polycrystalline calcite, usually coaxial and with $\sigma_1 > \sigma_2 = \sigma_3$, leads to an axially symmetric texture which can be completely characterized by one inverse pole figure for the shortening direction (Fig. 2). Within the range of experimental conditions where twinning is of major importance (low T, high stress) the axis of shortening rapidly rotates towards the c- and e axis directions in an inverse pole figure representation (Wenk *et al.* 1973; Casey *et al.* 1978, Spiers 1979). Wenk *et al.* (1973) attribute this texture to the combined effect of e-twinning and r-glide. Lister (1978), by computer simulation of texture development in calcite, found that a maximum near r develops if f-glide is as equally easy as r-glide, combined with a lower resolved shear stress for e-slip. This texture was found by Wenk *et al.* (1973) at higher temperatures and confining pressures.

At this point, it is important to stress the difficulties of comparing experimental data with our naturally deformed rocks which surely followed a rotational strain path (a strong component of simple shear is certainly indicated from field geological evidence). We know from experiments with $\sigma_1 \neq \sigma_2 \neq \sigma_3$ (Kern 1971) and from experiments simulating a rotational strain path (Rutter & Rusbridge 1977) that both the ratio of the magnitudes of the principal stresses and the strain path influence the resulting texture. Lister *et al.* (1978) came to the same conclusion based on texture simulation work.

Obliquity of textures

An attempt to interpret the oblique textures in specimens 7816 and 71 may be made with reference to the experiments of Rutter & Rusbridge (1977). By redeforming coaxially shortened marble which developed a strong c-axis maximum near the compression axis such that the previous shortening direction was oblique to the new σ_1 direction they found that the c-axis maximum rotates rapidly towards the new σ_1 direction. This results in the final c-axis maximum being oblique to the finite shortening axis. Their experiment may be qualitatively compared with a simple shear situation, where the short axis of the finite strain ellipsoid continuously rotates away from σ_1. It might then be expected that the c-axis would rotate away from the foliation normal (assumed to be essentially parallel to the Z-axis of the strain ellipsoid) towards σ_1, a situation compatible with our observations and known sense of shear found in specimens 7816 and 71. Rutter & Rusbridge (1977) suggested that this obliquity arises because the texture rapidly "forgets" its earlier deformation history (after only 35% shortening). The obliquity between grain elongation and finite strain observed in our specimen, as well as the discrepancy between the amount of flattening in pebbles and matrix grains (specimen 71) suggest that grain shape as well as texture may only record the last strain increments. These features are probably due to grain boundary migration and/or syntectonic recrystallization.

As a consequence of this interpretation, flattening perpendicular to the foliation during the last increments of strain must be postulated for specimen 7822, although positive field evidence for this is missing. Calcite c-axis maxima oriented oblique to the foliation normal have been observed in other naturally occurring deformed rocks (Wenk *et al.* 1968; Wenk & Shore 1975). The sense of obliquity may eventually be used as a useful criterion to infer unknown transport direction and sense of shear if more data should confirm the interpretation offered here.

Comparison with experiments

A direct comparison between inverse pole figures from experimentally, coaxially deformed specimens and the inverse pole figures of Fig. 2 must be restricted to inverse pole figures derived for those specimen directions which were parallel to σ_1 during the last strain increments. The high degree of symmetry around the direction of the c-axis maximum, combined with the observation from experiments that texture may only record the final increments of strain (Rutter & Rusbridge 1977), suggests that it is probably the c-axis maximum that coincides with the direction of σ_1 during the last strain increments. Parallelism between the c-axis maximum and σ_1, would then indicate, by analogy with experimental data, that *e*-twinning and *r*-glide were the major deformation mechanisms leading to the texture development.

Deformation mechanisms in the Lochseiten mylonite

The weak texture in the Lochseiten mylonite samples 6 and 115 suggests superplastic flow with grain boundary sliding as the dominant deformation mechanism (Schmid *et al.* 1977), a mechanism which would have been favoured by the extremely small grain size found in both these specimens and in the matrix of specimen 63. The microstructure of specimen 63 (Fig. 4d) suggests that this small grain size is the product of syntectonic recrystallization of the larger intraclasts deforming by *e*-twinning and glide possibly on *r* and *f*. Such a recrystallization-induced change in deformation mechanism in the Lochseiten mylonite would have dramatically weakened this lubricating layer (Schmid *et al.* 1977) and could explain the observation that shear was confined to this extremely thin mylonite horizon in the Glarus region.

ACKNOWLEDGMENTS. We are grateful to H. J. Möck from Scintag for providing the control software on the texture goniometer. F. Pirovino and E. Schärli prepared the samples and thin sections. J. Barber, Leeds, kindly provided specimen 71. The advice of A. Siddans, Leeds, in designing the texture goniometer used in this study was very helpful. J. S. would like to thank J. G. Ramsay for an invitation to spend a sabbatical leave in his department and to thank the ETH to make the visit possible. We thank O. A. Pfiffner for critically reading the manuscript. Field work was supported by the Swiss National Science Foundation (grant 2.859–0.77).

References

BADOUX, H. 1972. Tectonique de la nappe de Morcles entre Rhone et Lizerne. *Beitr. geol. Karte Schweiz*, **143,** 1–78.

BUNGE, H. J. 1969. *Mathematische Methoden der Texturanalyse.* Akademie Verlag, Berlin, 330 p.

—— & WENK, H. R. 1977. Three dimensional analysis of three quartzites (trigonal crystal and triclinic specimen symmetry). *Tectonophysics* **40,** 357–85.

CARTER, N. L. 1976. Steady state flow of rocks. *Rev. Geophys. Space Phys.* **14,** 301–60.

CASEY, M., RUTTER, E. H., SCHMID, S. M., SIDDANS, A. W. B. & WHALLEY, J. S. 1978. Texture development in experimentally deformed calcite rocks. *Proc. 5th Int. Conf. on Textures of Materials,* Springer Verlag, Berlin, 231–40.

KERN, H. 1971. Dreiaxiale Verformungen an Solnhofen Kalkstein im Temperaturbereich von 20°C–650°C. *Contrib. Mineral. Petrol.* **31,** 39–66.

LISTER, G. S. 1978. Texture transitions in plastically deformed calcite rocks. *Proc. 5th Int. Conf. on Textures of Materials,* Springer Verlag, Berlin, 199–210.

——, PATERSON, M. S. & HOBBS, B. E. 1978. The simulation of fabric development in plastic deformation and its application to Quartzite: The model. *Tectonophysics,* **45,** 107–58.

RUTTER, E. H. & RUSBRIDGE, M. 1977. The effect of non-coaxial strain paths on crystallographic preferred orientation development in the experimental deformation of a marble. *Tectonophysics,* **39,** 73–86.

SCHMID, S. M. 1974. The Glarus overthrust: Field evidence and mechanical model. *Eclog. geol. Helv.* **68,** 247–80.

——, BOLAND, J. N. & PATERSON, M. S. 1977. Super-plastic flow in fine-grained limestone. *Tectonophysics,* **43,** 257–91.

SIDDANS, A. W. B. 1976. Deformed rocks and their textures. *Philos. Trans. R. Soc. London.* **A. 283,** 43–54.

SPIERS, C. J. 1979. Fabric development in calcite polycrystals deformed at 400°C. *Bull. Minéral.* **102,** 282–89.

WENK, H. R. & SHORE, J. 1975. Preferred orientation in experimentally deformed dolomite. *Contrib. Mineral. Petrol.* **50,** 115–26.

——, TROMMSDORFF, V. & BAKER, D. W. 1968. Inverse pole figures of two carbonate fabrics. *Schweiz. mineral. petrogr. Mitt.* **48,** 467–70.

——, VENKITASUBRAMANYAN, C. S. & BAKER, D. W. 1975. Preferred orientation in experimentally deformed limestone. *Contrib. Mineral. Petrol.* **38,** 81–114.

S. M. SCHMID, Geologisches Institut der ETH, Zürich, Switzerland.
M. CASEY, Department of Earth Sciences, The University, Leeds, England.
J. STARKEY, Geology Department, University of Western Ontario, London, Ontario, Canada.